MEMORANDUM

From	:	Pauline Cocevar and Siân O'Hara	**Document Ref**	:	IDEAS-VEG-OQC-REP-1490
To	:	Philippe Goryl	**Date**	:	04 September 2014
			Issue	:	1.1; Fig.7 corrected
cc.	:	AATSR QWG aatsr@eo-sppa.org	**File ID**	:	IDEAS-VEG-OQC-REP-1490 AATSR Colocation Review v1-1.doc

SUBJECT : AATSR Colocation Review

This report contains a case-study review of the AATSR nadir/forward view colocation after the third full reprocessing.

Scope

The 3rd reprocessing of the full AATSR dataset contained updates to improve both absolute nadir geolocation and nadir/forward view colocation (also called coregistration); these updates were implemented via changes to the CH1 auxiliary data file (ADF), and the improvements were confirmed as part of the quality control (QC) on the reprocessed dataset. This report presents a further assessment, using a set of case studies, to double check the improvement and also to attempt to highlight any anomalies that may still exist.

Background

Spot-check analysis, as well as systematic QC, was carried out on the AATSR 3rd reprocessing dataset [1]. The colocation assessment was based on difference (forward–nadir) statistics and difference images using the 0.87 μm visible channel. These were large-scale assessments of several products and confirmed an improvement in the colocation. Improvement in the absolute nadir geolocation was also confirmed.

It was noted, however, that the colocation improvement shown in earlier test data received from RAL had not been fully realised in the 3rd reprocessing dataset [2]. A subsequent investigation by RAL [3] found that the iterative technique to optimise the CH1 ADF had been carried out using predicted orbit state vectors (OSVs) propagated throughout the orbits, rather than restituted OSVs, and that it was likely that the updated CH1 was not fully optimal when using restituted OSVs (as is the case within ESA's Instrument Processing Facility).

An earlier analysis [4] of colocation on the 2nd reprocessing dataset (using the 11 and 12 μm bands) demonstrated different optimum view shifts for AATSR, depending on time and across-track position.

AATSR instrument

Full details of the AATSR instrument are outlined in the AATSR Handbook [5]. Section 3.2.1.2 gives information on the <u>curved</u> ~500-km wide swaths, which contain 555 pixels across the nadir swath and 371 across the forward swath. The nominal instantaneous field of view (IFOV) is 1 x 1 km at the centre of the nadir swath, but 1.5 x 2 km at the centre of the forward swath, due to the angle at which it is projected onto the Earth. Section 2.12.1.7 of the AATSR Handbook displays the true IFOV on the ground for the 11 μm channel: figure 2.15 shows how it extends beyond the edges of the 1-km square pixel even at the centre of the nadir swath, and how this extension is increased for the forward view at the centre of its swath and also for both views as the instrument scans along the curve. For homogeneous surfaces such as open ocean, these distortions are not very important, but users should be aware of this effect, especially for forward/nadir view comparisons and work carried out over heterogeneous surfaces (e.g. LST applications).

Case studies

Comparisons of data from the 2nd and 3rd reprocessings of AATSR were carried out using the 12 µm brightness temperature (BT) channel rather than the 0.87 µm reflectance channel (so as to perform this analysis on one of the same bands as used in [4]). A number of specific sites with a relatively small surface area were selected to try to gain some understanding of the changes that have been made to the colocation between the 2nd and 3rd reprocessings. Details of the selected sites are given in Table 1.

Table 1. Case study sites

Site	Type	Location		Across-track pixel no.	Approx. dimensions (km)	Satellite image of site (©Google)
		Lat.	Lon.			
Kalmar strait	island	57.2519	16.7925	330	0.9 x 1.1	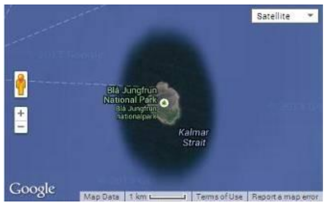
Linosa	island	35.8661	12.8687	164	2.8 x 2.3	
Hoedic	island	47.3391	-2.8749	264	2.3 x 1.9	
Lake Aluksne	lake	57.4531	27.0840	254	4.6 x 4.9	
Lake Otno	lake	59.1615	36.4515	275	3.7 x 3.4	

The BEAM images shown in the following subsections for each of the test sites display 12 µm BTs for comparison: the top row is the 2nd reprocessing product, the bottom row is the 3rd reprocessing product. Forward views are on the left and nadir views are on the right. The pin in each figure is at the location of the site specified in Table 1. All four images within any one figure are displayed on the same colour scale, highlighting the differences in values that are reported from the forward and nadir views for the same feature. Note that the feature is viewed first in the forward view at an angle of 55°, and then 150 seconds later (approximately 1000 km forward along the ground track), a second observation is made of the same feature at the sub-satellite point in the nadir view.

Kalmar strait

Identification of an approximately 1 x 1 km island in the Kalmar strait gives an illustration of the difficulties in trying to detect small features in the AATSR products and in comparing the forward and nadir views of the features.

The products displayed in Figure 1 for the island in the Kalmar strait are:

[1] ATS_TOA_1PRUPA20030329_091518_000065272015_00064_05629_7309.N1
[2] ATS_TOA_1PUUPA20030329_091523_000065272015_00064_05629_9059.N1

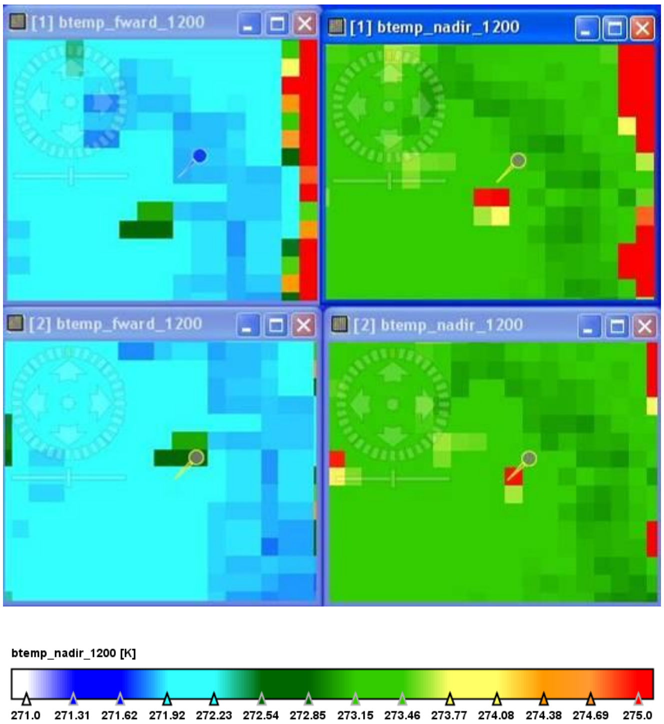

Figure 1. BEAM image of the 12 µm brightness temperatures for the 2nd (top) and 3rd reprocessings (bottom) of AATSR for the island in Kalmar strait. Left: forward view; right: nadir view. The pin is at the location of the island specified in Table 1.

The 2nd reprocessing nadir view (top right) shows that the signal from the 1-km island covers 4 pixels in the product, and not 1 pixel as might be initially expected. For the 3rd reprocessing, the signal now covers 2 pixels (bottom right); the difference being due to changes in how gridding fell between the two reprocessings. There is, however, a single “hot spot” pixel for this product in the 3rd reprocessing product. The location of the island relative to the pin demonstrates the improved absolute nadir geolocation for the 3rd reprocessing. Inspection of the forward views shows that the signal from the island covers 5 pixels, unchanged between the reprocessings. The shift in the forward view is quite considerable (2 pixels across track and 4 pixels along track) for the 3rd reprocessing product; the pin is now closer to the identified island, approximately central across track, but there is a case to be made that the shift was too far along track.

Linosa

Linosa was chosen as a case study site since it featured in the colocation assessment carried out in [4], which examined in detail the colocation errors of all (A)ATSR instruments in the 11 and 12 μm channels for products from the 2nd reprocessing.

Two different orbits were chosen for Linosa, both since this island was a site featuring in the earlier study [4] and to illustrate the different signatures that the same feature can generate in AATSR products.

The products displayed in Figure 2 for Linosa are:

[1] ATS_TOA_1PRUPA20080516_084635_000065272068_00350_32468_7506.N1
[2] ATS_TOA_1PUUPA20080516_084635_000065272068_00350_32468_5703.N1

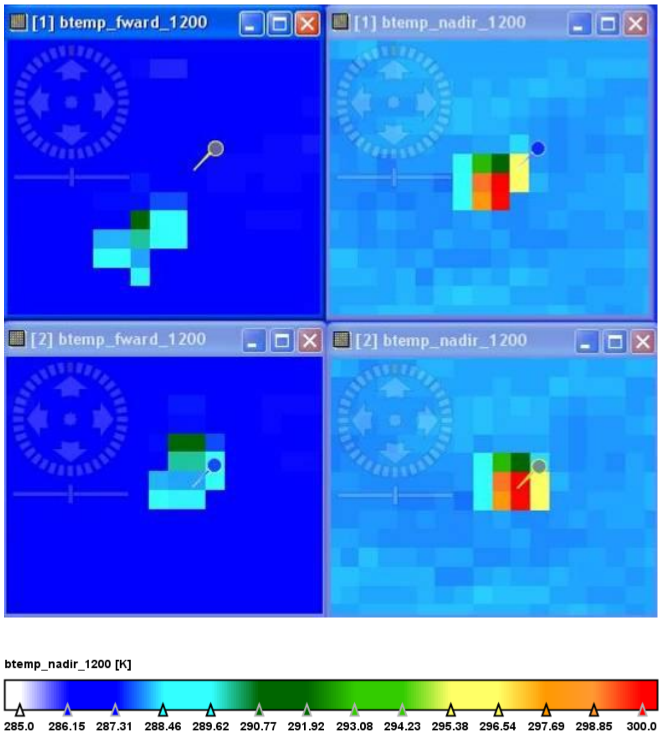

Figure 2. BEAM image of the 12 μm brightness temperatures for the 2nd (top) and 3rd reprocessings (bottom) of AATSR for Linosa, orbit 32468. Left: forward view; right: nadir view. The pin is at the location of the island specified in Table 1.

Since Linosa is larger than the Kalmar strait island, the signal from Linosa is spread over many more pixels. Nadir geolocation looks to be improved for the 3rd reprocessing, with the centre of the identified feature closer to the pin. The shape of the forward view image of Linosa changed considerably between the 2nd and the 3rd reprocessings, but the identified feature now contains the pin within it, approximately at the across-track centre. Again, it would seem that the shift was too far along track.

The products displayed in Figure 3 for Linosa are:

[3] ATS_TOA_1PRUPA20080706_084344_000065272070_00078_33198_2058.N1
[4] ATS_TOA_1PUUPA20080706_084344_000065272070_00078_33198_6441.N1

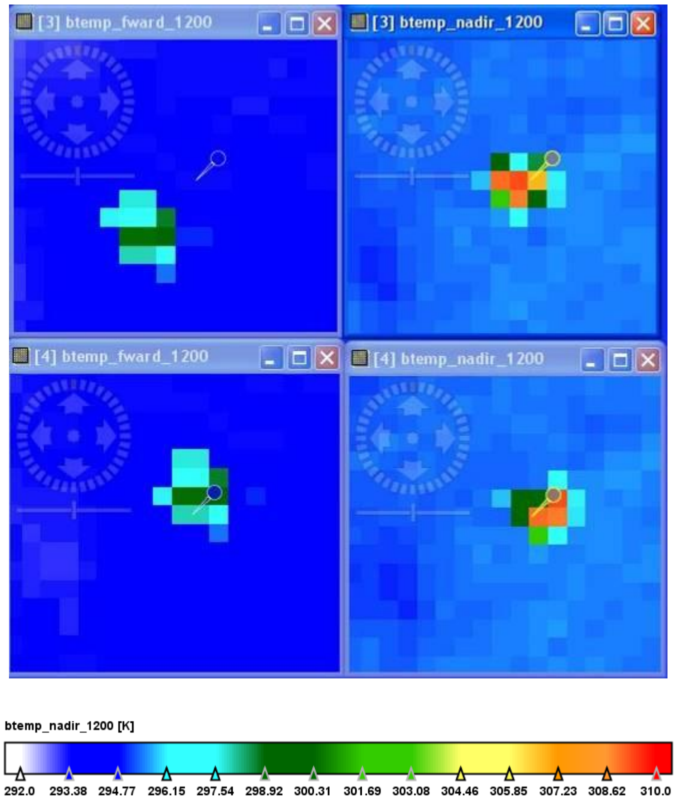

Figure 3. BEAM image of the 12 µm brightness temperatures for the 2nd (top) and 3rd reprocessings (bottom) of AATSR for Linosa, orbit 33198. Left: forward view; right: nadir view. The pin is at the location of the island specified in Table 1.

In Figure 3, the shapes of Linosa in the forward-view images of the 2nd and 3rd reprocessings are similar, however the identified feature for the 3rd reprocessing now contains the pin, whereas the feature in the 2nd reprocessing product did not. There is no clear visible improvement in nadir geolocation for this example.

Hoedic

The products displayed in Figure 4 for Hoedic are:

[1] ATS_TOA_1PRUPA20090318_100954_000065272077_00222_36849_8588.N1
[2] ATS_TOA_1PUUPA20090318_100954_000065272077_00222_36849_0254.N1

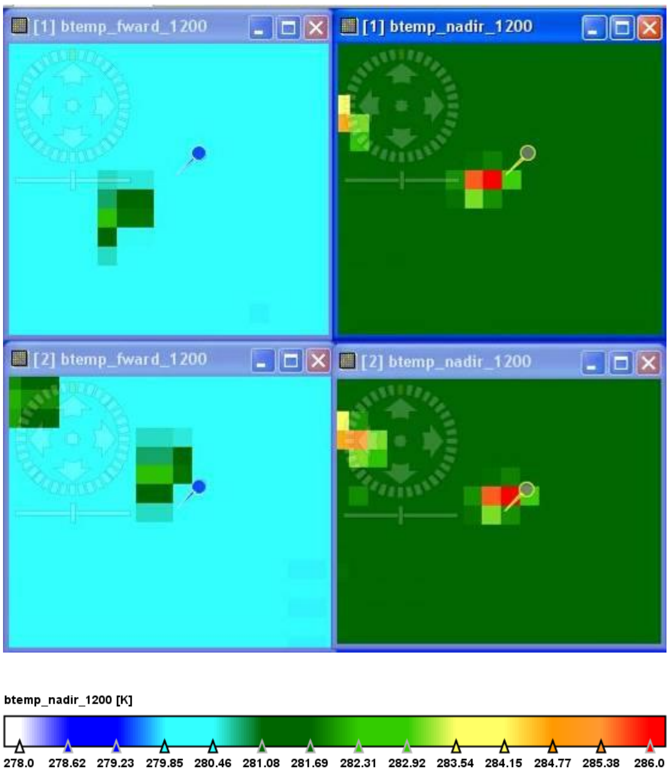

Figure 4. BEAM image of the 12 µm brightness temperatures for the 2nd (top) and 3rd reprocessings (bottom) of AATSR for Hoedic. Left: forward view; right: nadir view. The pin is at the location of the island specified in Table 1.

It can be seen in Figure 4 that the absolute nadir geolocation has changed, although the improvement for the 3rd reprocessing is less obvious from visual inspection (cf. results in next section: Centres of features: forward and nadir centres vs pin location). The forward view feature is largely unchanged in shape between the products, with the location generally improved in the 3rd reprocessing, but it still could not be considered satisfactory.

Lake Aluksne

As well as inspecting island sites (warm spots against a cooler background), a couple of lake sites were chosen to provide the opposing perspective. For small lakes (~4 pixels in the nadir view), it was difficult to discern the relevant signal in the forward view, so the chosen lakes were by necessity larger than the island test sites.

The products displayed in Figure 5 for Lake Aluksne are:

[1] ATS_TOA_1PRUPA20100512_082911_000065272089_00221_42860_8954.N1
[2] ATS_TOA_1PUUPA20100512_082911_000065272089_00221_42860_6736.N1

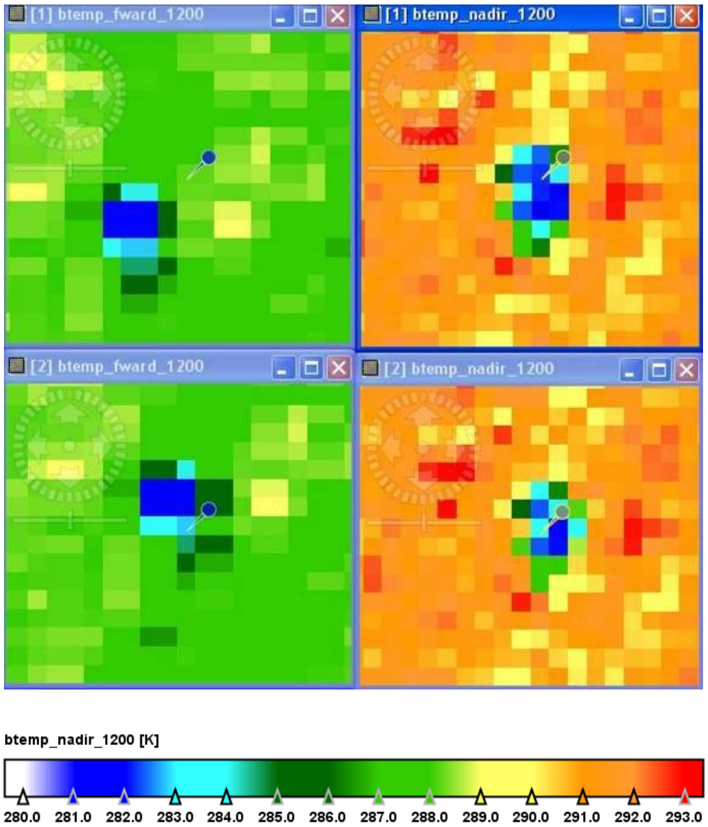

Figure 5. BEAM image of the 12 µm brightness temperatures for the 2nd (top) and 3rd reprocessings (bottom) of AATSR for Lake Aluksne. Left: forward view; right: nadir view. The pin is at the location of the lake specified in Table 1.

In common with the pattern seen for most of the previous sites, the nadir geolocation can be considered to be improved in the 3rd reprocessing products, and the identified feature for the 3rd reprocessing in the forward view is better positioned relative to the pin than in the 2nd, although not perfectly sited.

Lake Otno

The products displayed in Figure 6 for Lake Otno are:

[1] ATS_TOA_1PRUPA20100513_075734_000065272089_00235_42874_3966.N1
[2] ATS_TOA_1PUUPA20100513_075734_000065272089_00235_42874_6750.N1

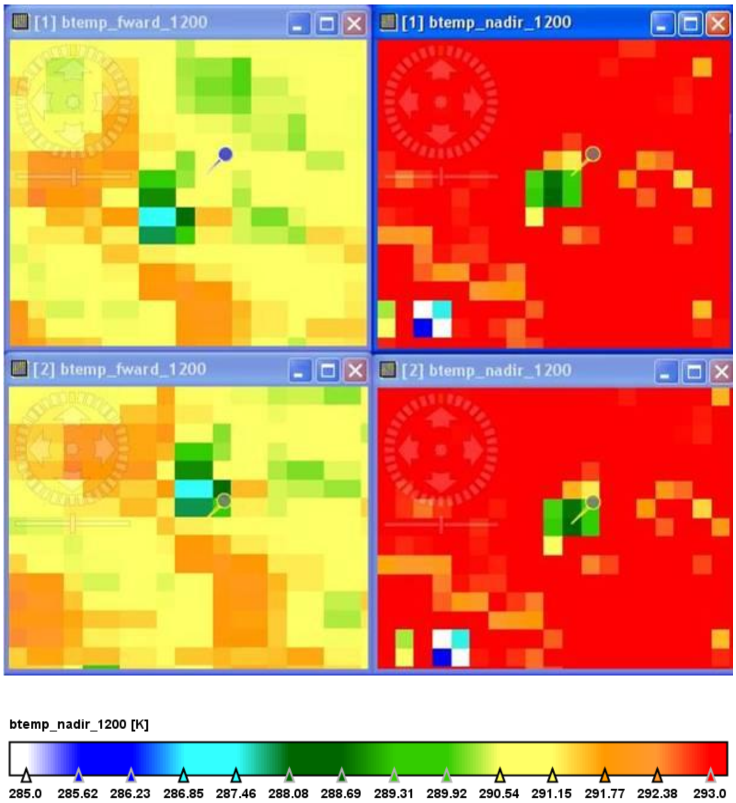

Figure 6. BEAM image of the 12 µm brightness temperatures for the 2nd (top) and 3rd reprocessings (bottom) of AATSR for Lake Otno. Left: forward view; right: nadir view. The pin is at the location of the lake specified in Table 1.

For Lake Otno it can again be seen that there was a considerable, again perhaps too large, shift in the forward view colocation, although the feature is now approximately central to the pin across track. The nadir geolocation again looks to be improved in the 3rd reprocessing image.

Centres of features: forward and nadir centres vs pin location

For each of the case studies, an estimate was taken of the centre of the identified feature in both views. A weighted average (using the 12 µm BT) of the centre locations of the pixels making up each feature was calculated, and then the distance from this centre location to the pin location was measured. Table 2 displays the distance (in km) of the centre location of the feature from the pin location for all sites, for both views and for 2nd and 3rd reprocessing data products. The average distance for the six sites is also given. There is a clear improvement in both views for all sites, with the exception of the forward view for Lake Otno, where there is hardly any change. The information in Table 2 is displayed in Figure 7 and Figure 8.

Table 2. Distance (km) of feature centre from the pin location

Site name	Site no.	Forward view			Nadir view		
		2nd reprocessing	3rd reprocessing	% change	2nd reprocessing	3rd reprocessing	% change
Kalmar	1	2.89	1.65	43%	1.36	0.47	66%
Linosa 32468	2	4.50	0.76	83%	1.45	0.42	71%
Linosa 33198	3	3.88	1.10	72%	0.86	0.38	56%
Hoedic	4	3.17	2.16	32%	1.02	0.67	34%
Aluksne	5	4.01	1.24	69%	1.11	0.49	56%
Otno	6	2.50	2.49	0%	1.13	0.48	58%
Average		**3.49**	**1.57**	**55%**	**1.16**	**0.49**	**58%**

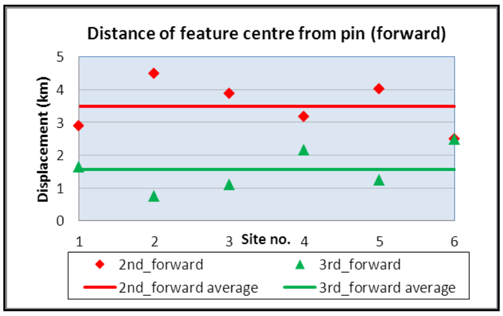

Figure 7. Distance of feature centre from the pin location for the forward view

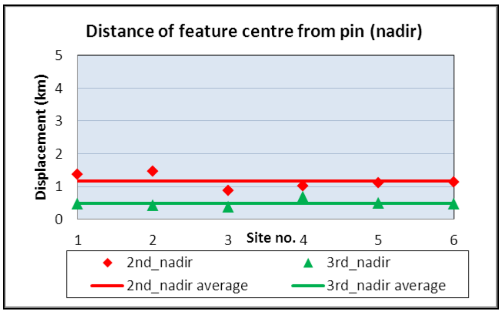

Figure 8. Distance of feature centre from the pin location for the nadir view

Whereas the improvement in the nadir view location is fairly consistent across all the sites, there is a large variation when this method is applied to the forward views. On average, there is a clear improvement, but the improvements for the individual sites are quite different, especially for the forward view as can clearly be seen from Figure 7.

The change in the forward view of Lake Otno (site no. 6) demonstrates the smallest (in fact negligible) improvement: Table 2 and Figure 7 show that the distance from the feature centre to the lake location has barely changed between the two reprocessings, despite a visual inspection from Figure 6 suggesting the feature is better located with respect to the pin. Figure 9 gives a closer view of the lake location and the weighted feature centre, where the left image is the forward view from the 2nd reprocessing and the right image is from the 3rd.

Figure 9. BEAM image of the forward-view 12 µm brightness temperatures for the 2nd (left) and 3rd reprocessings (right) of AATSR for Lake Otno. The Lake Otno pin is at the location specified in Table 1; the 2nd_Centre and 3rd_Centre pins are at the weighted centre of the image feature.

It can be seen from Figure 9 that, although the across-track location of the feature has markedly improved relative to the pin location, the along-track location of the feature is now more than 2 pixels from the pin location. Visual inspection of the images for the other locations feature an along-track displacement of roughly 1 pixel, or slightly more.

The results above illustrate that any attempt to improve the colocation must be taken from an assessment of a large set of products, ranging in both location and time.

Centres of features: forward–nadir distance

The previous section analysed the weighted centre of the features in each view and demonstrated improvements in their distances from the independent pin locations. This section analyses the forward–nadir distance of the weighted centres of the features for each of the reprocessings.

Table 3 and Figure 10 show the forward–nadir distance (km) between the weighted centre of the features for the 2nd and 3rd reprocessings.

Table 3. Distance (km) between the weighted centres of the forward and nadir features for the 2nd and 3rd reprocessings

Site name	Site no.	Forward–nadir distance (km)		
		2nd reprocessing	3rd reprocessing	% change
Kalmar	1	1.72	1.93	-12%
Linosa 32468	2	3.37	0.49	86%
Linosa 33198	3	3.08	1.00	68%
Hoedic	4	2.18	1.56	29%
Aluksne	5	3.02	1.32	56%
Otno	6	1.40	2.01	-44%
Average		**2.46**	**1.38**	**44%**

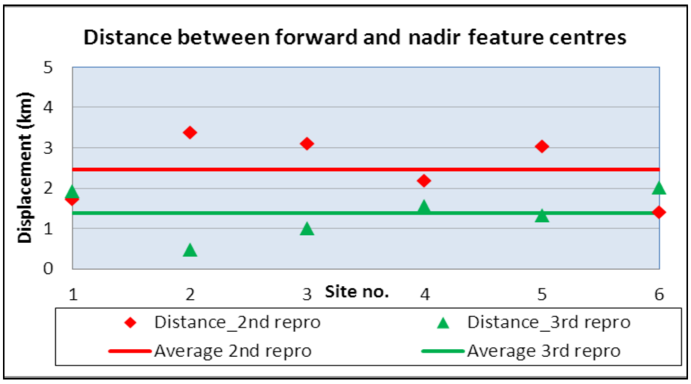

Figure 10. Distance (km) between the weighted centres of the forward and nadir features for the 2nd and 3rd reprocessings.

It can be seen from Table 3 that there has been an average improvement over all six sites, showing that the colocation has improved on the whole. However, two of the six sites (Kalmar and Otno) now show a greater distance between the forward and nadir feature centres in the 3rd reprocessing than they did in the 2nd reprocessing. In percentage terms, the change in forward–nadir distances are very variable, with the two Linosa sites showing improvements of 68 and 86%, while the Kalmar and Otno features deteriorate by 12 and 44%, respectively.

The results presented above would again appear to show that results from a small number of analysed products must be viewed with caution, and that the best analysis of colocation status needs a comprehensive set of test products.

Forward–nadir difference in the 0.87 µm band

Statistical differences

The method outlined in [1], using a comparison of the forward–nadir difference values in the 0.87 µm band, was repeated for the products inspected in this report. The 0.87 µm difference statistics were calculated for a full-width 512 x 512 pixel scene around each site, and also for each product as a whole. The intention was to investigate whether the changes in differences for each scene were representative of the whole product.

Table 4 displays the mean of the 0.87 µm band forward–nadir differences for scenes around each site and for the whole products.

Table 4. Mean of 0.87 µm band forward–nadir differences for site scenes and whole products

Site	Site no.	512 x 512 scene			Whole product		
		2nd repro	3rd repro	% change	2nd repro	3rd repro	% change
Kalmar	1	3.91	3.86	1%	2.51	2.44	3%
Linosa 32468	2	-3.42	-3.23	5%	3.25	3.01	7%
Linosa 33198	3	-5.19	-4.85	6%	3.15	2.92	7%
Hoedic	4	2.48	2.21	11%	2.91	2.68	8%
Aluksne	5	2.11	1.95	8%	3.53	3.28	7%
Otno	6	0.59	0.58	3%	3.38	3.14	7%
Average		**2.95**	**2.78**	**6%**	**3.12**	**2.91**	**7%**

Note that Linosa scene difference values in Table 4 were negative; the absolute values were used when calculating percentage change and averages. Positive percentage changes demonstrate improvement.

Table 4 shows an improvement in the mean difference values (i.e. the difference is closer to zero) for all site scenes and all products for the 3rd reprocessing dataset. While the percentage improvement for 512 x 512 pixel scenes varies from 1 to 11%, the average value of 6% is very close to the average value for the whole product (7%). The changes for the whole products are more consistent (3–8%), as might be expected with the statistics being calculated over ~16 million pixels, rather than approximately 260,000 as for the site scenes.

Table 5 displays the standard deviation of the 0.87 µm band forward–nadir differences for scenes around each site and for the whole products. Again, there are improvements in all cases for the 3rd reprocessing dataset, and the average improvement in the site scenes (14%) is close to that for the whole products (17%). The individual site scenes again display a large variability compared with the whole products.

Table 5. Standard deviation of 0.87 µm band forward–nadir differences for site scenes and whole products

Site	Site no.	512 x 512 scene			Whole product		
		2nd repro	3rd repro	% change	2nd repro	3rd repro	% change
Kalmar	1	3.19	3.01	6%	6.17	5.00	19%
Linosa 32468	2	5.37	4.83	10%	8.02	6.55	18%
Linosa 33198	3	6.80	6.23	8%	8.64	7.10	18%
Hoedic	4	2.74	2.19	20%	7.09	5.75	19%
Aluksne	5	6.09	4.98	18%	8.16	6.94	15%
Otno	6	5.24	4.22	19%	7.73	6.71	13%
Average		**4.91**	**4.24**	**14%**	**7.63**	**6.34**	**17%**

The values in Table 4 and Table 5 are displayed graphically in Figure 11 to Figure 14.

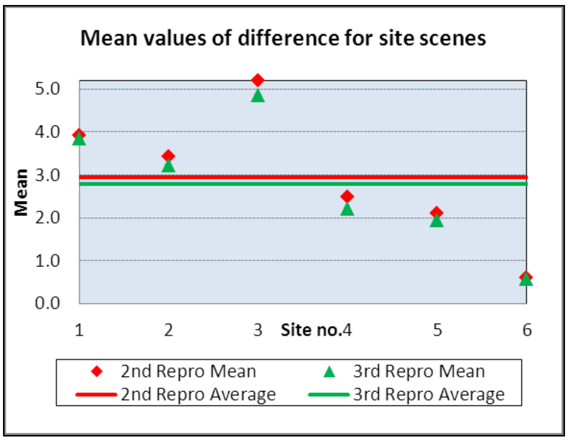

Figure 11. Mean of forward–nadir view difference for site scenes.

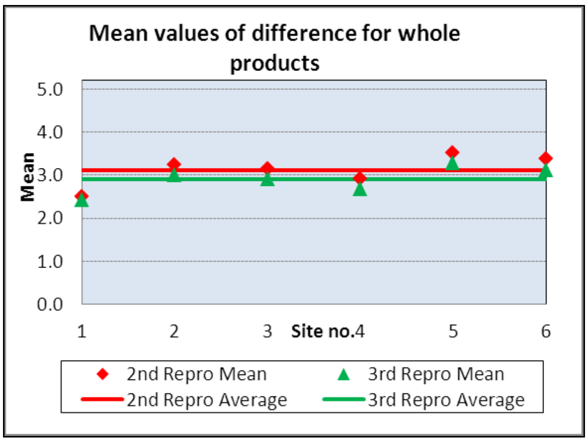

Figure 12. Mean of forward–nadir view difference for whole products.

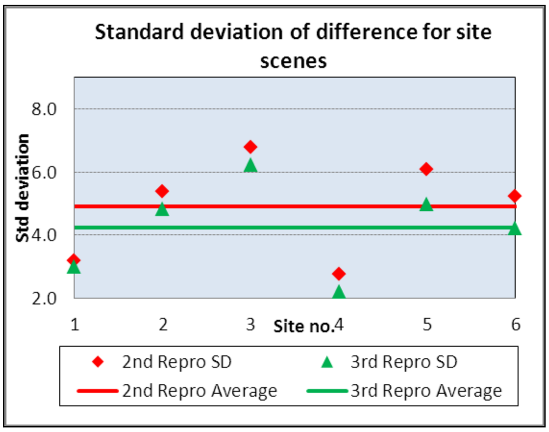

Figure 13. Standard deviation of forward–nadir view difference for site scenes.

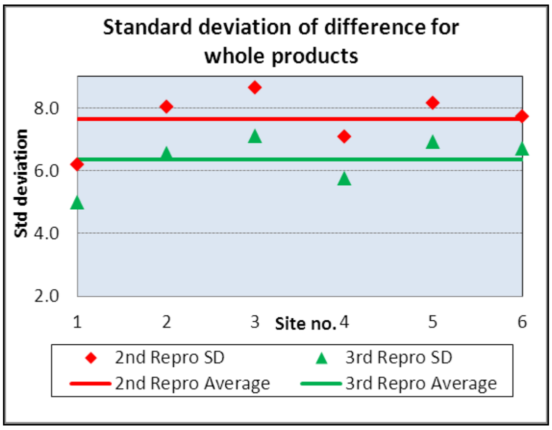

Figure 14. Standard deviation of forward–nadir view difference for whole products.

Site scenes

The forward–nadir statistical differences for the site scenes in Table 4 and Table 5 are quite different for each site; the whole products are more consistent with each other. This is due to the nature of the chosen scenes, which can be quite different. Differences between the two views will be larger if the scene is relatively heterogeneous. Figure 15 to Figure 20 show images of the scenes for each of the sites: on the left is the 0.87 μm difference image from the 2nd reprocessing; on the right is that from the 3rd reprocessing. Large forward–nadir 0.87 μm differences can be easily seen (as black or white pixels) for certain features, such as coastlines, lake edges, cloud edges/shadows.

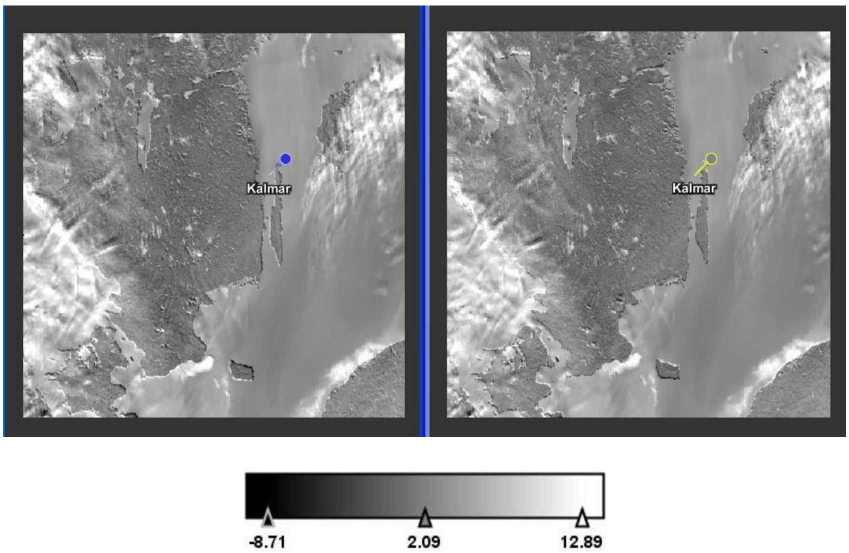

Figure 15. The forward–nadir difference image (0.87 μm) for 2nd reprocessing data (left) and 3rd reprocessing data (right) for a 512 x 512 pixel scene around the island in the Kalmar strait.

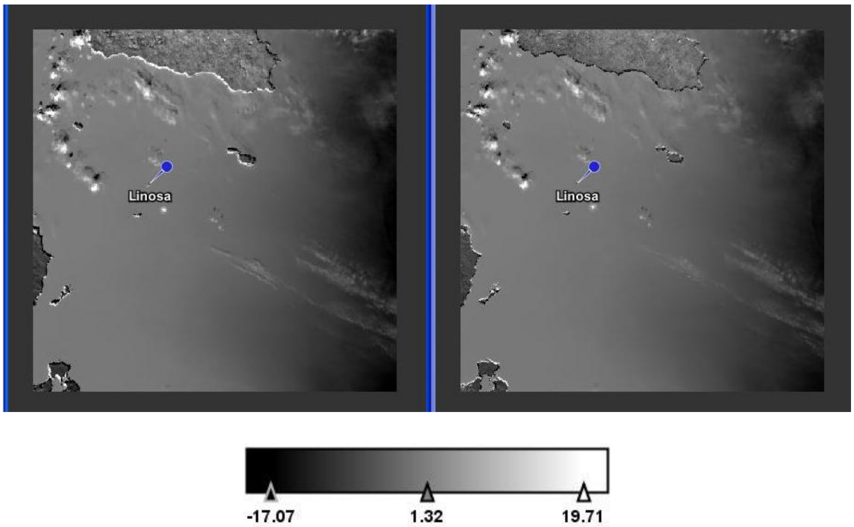

Figure 16. The forward–nadir difference image (0.87 µm) for 2nd reprocessing data (left) and 3rd reprocessing data (right) for a 512 x 512 pixel scene around Linosa (orbit 32468).

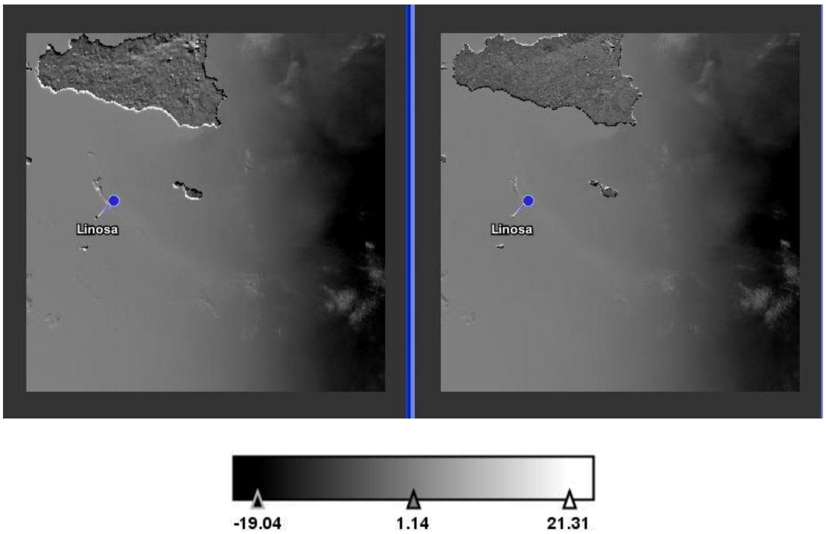

Figure 17. The forward–nadir difference image (0.87 µm) for 2nd reprocessing data (left) and 3rd reprocessing data (right) for a 512 x 512 pixel scene around Linosa (orbit 33198).

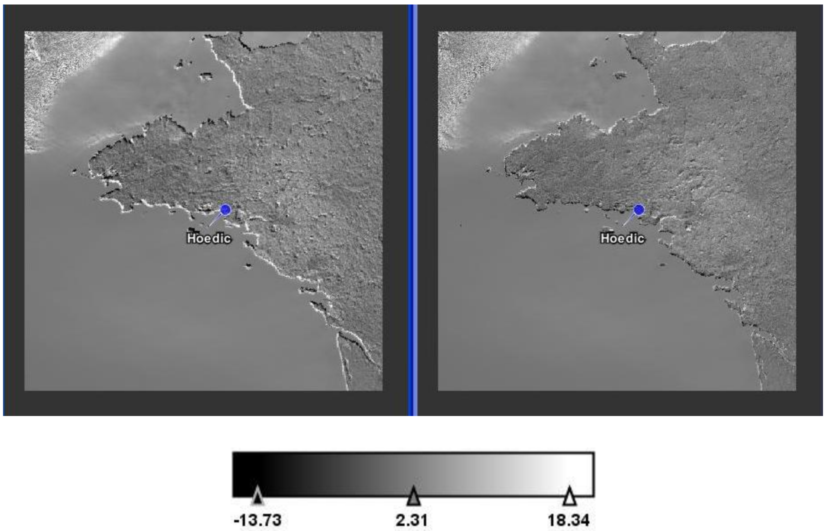

Figure 18. The forward–nadir difference image (0.87 μm) for 2nd reprocessing data (left) and 3rd reprocessing data (right) for a 512 x 512 pixel scene around Hoedic.

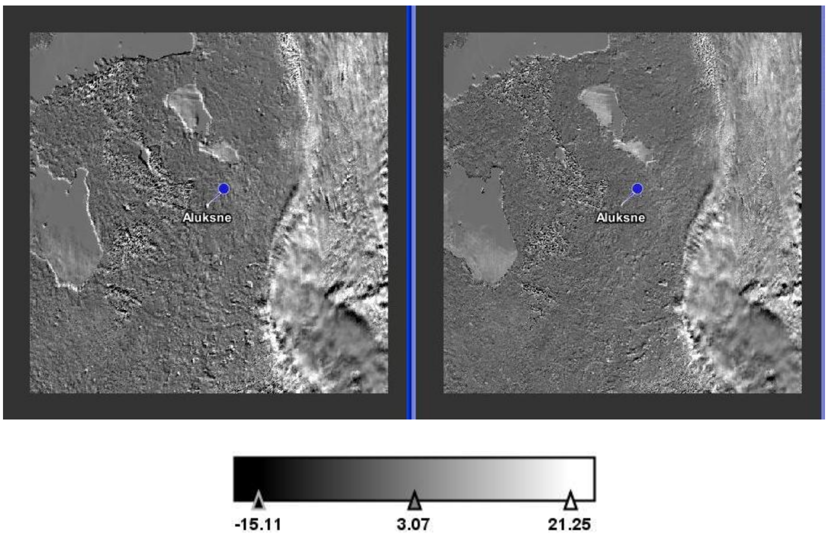

Figure 19. The forward–nadir difference image (0.87 μm) for 2nd reprocessing data (left) and 3rd reprocessing data (right) for a 512 x 512 pixel scene around Lake Aluksne.

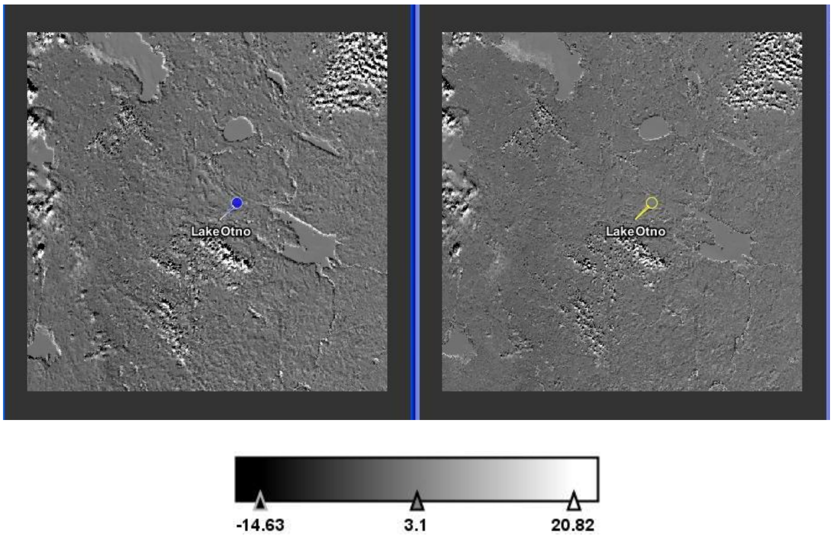

Figure 20. The forward–nadir difference image (0.87 μm) for 2nd reprocessing data (left) and 3rd reprocessing data (right) for a 512 x 512 pixel scene around Lake Otno.

Comparison with reprocessed QC

The difference statistics from the Reprocessing QC [1], which were for 22 whole products covering the AATSR mission, are given in Table 6. Also given in Table 6 are the difference statistics for the case study whole products (reproduced from Table 4 and Table 5).

Table 6. Average view difference mean and standard deviation for 2nd and 3rd reprocessing AATSR data for 22 products covering the AATSR mission and for the case study whole products

		2nd repro	3rd repro	% change
Average mean	Reprocessing QC	2.76	2.60	6%
	Case study whole products	3.12	2.91	7%
Average standard deviation	Reprocessing QC	7.83	6.50	17%
	Case study whole products	7.63	6.34	17%

The results for the forward–nadir differences shown in Table 6 are in broad agreement, showing almost the same relative improvement in the mean and standard deviation. This serves to confirm the results reported in [1] and offers reassurance that this method of evaluating colocation improvements is robust and representative, as long as a large enough number of products are assessed.

Visual assessment

The improvement can also be noted visually in images of the difference band, as shown in a close-up image from the Hoedic products in Figure 21. The image for the 2nd reprocessing data has much more variation, indicating more difference, whereas the image for the 3rd reprocessing data is much "flatter" meaning there is less difference and so the views are better colocated. These features were also visible in the scene images in Figure 15 to Figure 20.

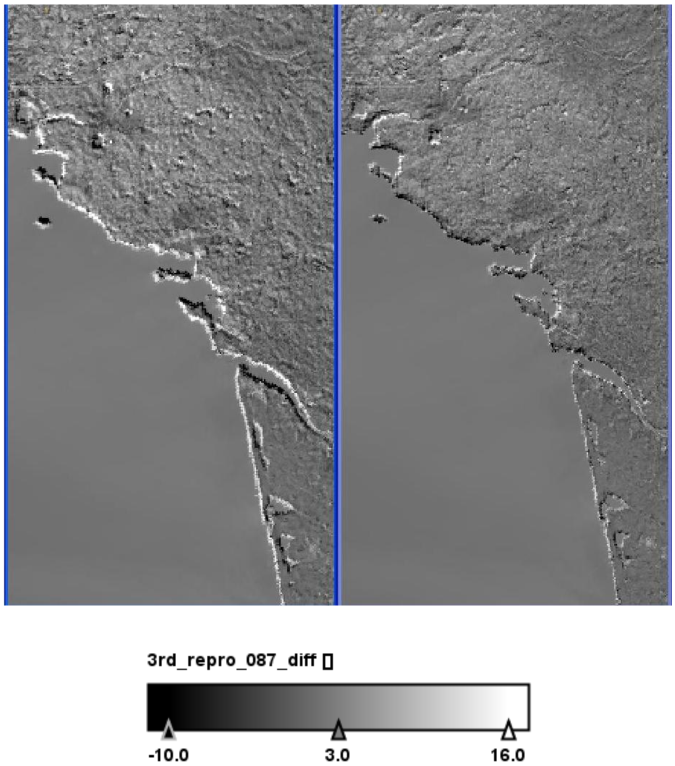

Figure 21. The forward-nadir difference image (0.87 µm) for 2nd reprocessing data (left) and 3rd reprocessing data (right) from the Hoedic products.

Although an overall visual improvement in colocation has been noted, closer analysis of, for example, Figure 17 (for Linosa, orbit 33198) demonstrates that the colocation can still be improved. By focussing on the southern coastline of Sicily, it can be noted that the band of white pixels in the 2nd reprocessing image have now been replaced by a band of black pixels. The along-track shift for this particular site appears to have been too large

Conclusions

The case study assessments of six small sites viewed in the 12 µm band confirm the improvement in colocation for the 3rd reprocessing with respect to the 2nd reprocessing. Visual assessment of the pixels representing each site showed that the identified feature is now nearly always closer to, and in some cases encompasses, the location of the site represented by the pin (Figure 1 to Figure 6). While the locations of the identified features have definitely improved, the figures appear to show that while the across-track positioning is now more appropriate, the along-track positioning is not quite correct.

The qualitative assessment of improvement was reinforced by the calculation of the weighted centre of each identified feature, and the calculation of its distance from the pin location (Table 2). All sites for both views showed a considerable improvement, with the sole exception of the forward view for Lake Otno (Figure 6), which demonstrated no change. For the six sites, the average distance of the forward view feature from the pin was reduced from 3.5 km to 1.6 km; the average distance of the nadir view feature from the pin was reduced from 1.2 km to 0.5 km. These results confirm previous assessments of improvements in geolocation for the 3rd reprocessing dataset. Assessment of the distances between the weighted centres of the features in the nadir and forward views proved more variable (Table 3). There was an average improvement in distances between the two views of 2.5 km to 1.4 km for all six sites, but two of the six sites showed an increase in the distance. Again, this confirms the general improvement in colocation, but also provides further evidence that there are still improvements to be made, as well as highlighting the variable nature of colocation analysis over small sites.

Forward–nadir difference statistics for the 0.87 μm band, replicating the analysis method applied to both operational data and the reprocessed dataset before release [1], were calculated for 512 x 512 pixel scenes in the location of the six small sites and for their whole products (Table 4 and Table 5). The statistics for the scenes were found to be very variable, but all showed improvement; those for the whole products were more consistent, and also showed improvement. The average relative improvements for the scenes and the whole products were consistent with those from the reprocessed dataset before release (Table 6), showing improvements in the mean to be 6–7% and improvements in the standard deviation to be 14–17% when compared with the statistics from the 2nd reprocessing dataset.

Visual inspections of the forward–nadir difference images provide an alternative method of assessment (Figure 15 to Figure 21). Taking the views as a whole, the images for the 2nd reprocessing data have much more variation, indicating more difference, whereas the images for the 3rd reprocessing data are much "flatter" meaning there is less difference and so the views are better colocated.

By focussing on coastline edges within the forward–nadir difference images (e.g. Figure 17), previous differences in the east–west coastline that showed up as a band of thick white pixels in the 2nd reprocessing are a band of thin black pixels in the 3rd reprocessing; those that were thick black bands are now thin white bands. This observation shows that the along-track colocation has reduced in magnitude but switched in sign, and reinforces the previous observation that the along-track shift has been too large.

Summary

The two different methods of colocation analysis confirm that the forward/nadir view colocation has improved in the 3rd reprocessing AATSR dataset when compared with the 2nd reprocessing. Both quantitative and qualitative assessments demonstrate the improvement, but there is evidence that the forward view has been shifted too far along track with respect to the nadir view. It had been noted earlier [2, 3] that further improvement in the colocation should be possible, and this is supported by the results of the analysis conducted in this assessment.

Results also show that it is considered advisable, when attempting to improve the colocation, to base assessments on a substantial number of products, ranging in location and time.

The analysis in [4] noted that any estimated across- or along-track shift can be dependent on across-track position, time and channel; this assessment is due to be repeated for 3rd reprocessing data.

The AATSR QWG agreed at the 29th meeting (held in March 2014) that there was scope for further improvement of the colocation [6], and aims to provide a definitive statement for users on colocation within the 3rd reprocessing dataset by autumn 2014.

Plans are already in hand, outlined in [3], to modify the CH1 ADF for the 4th reprocessing of AATSR and to try to improve the colocation further. There will also be improvements to the absolute nadir geolocation (via the use of orthogeolocation), which will feed into improved colocation.

Referenced Documents

[1] IDEAS, AATSR Third Reprocessing Detailed QC Report, v1.0, IDEAS-VEG-OQC-REP-1356, 08 October 2013.

[2] IDEAS, AATSR Third Reprocessing Colocation Memo, v1.0, IDEAS-VEG-OQC-MEM-1301, 06 August 2013.

[3] O. Oduleye, Third Reprocessing Colocation Issue, v0.2, PO-TN-RAL-AT-0562, 14 March 2014.

[4] S. Casadio, On (A)ATSR(-1/2) Co-Location, v0.2, 10 December 2010.

[5] AATSR Product Handbook, available at: https://earth.esa.int/handbooks/

[6] 29th AATSR Quality Working Group – Minutes of Meeting, v1.0, IDEAS-VEG-OQC-MIN-1472, 06 May 2014.